

Geophysical Research Letters

RESEARCH LETTER

10.1029/2019GL083177

Key Points:

- Extreme frontal, not tropical, storms caused fall precipitation in the southeastern United States to increase by approximately 40% during 1895–2018
- Mean intensity of daily precipitation drove the fall precipitation increase via increased frequency of extreme precipitation events
- Increased southerly moisture flux enhanced high-intensity precipitation more than lower-intensity precipitation

Supporting Information:

- Supporting Information S1

Correspondence to:

D. A. Bishop,
dbishop@ldeo.columbia.edu

Citation:

Bishop, D. A., Williams, A. P., & Seager, R. (2019). Increased fall precipitation in the southeastern United States driven by higher-intensity, frontal precipitation. *Geophysical Research Letters*, *46*, 8300–8309. <https://doi.org/10.1029/2019GL083177>

Received 4 APR 2019

Accepted 2 JUL 2019

Accepted article online 8 JUL 2019

Published online 22 JUL 2019

This article was corrected on 1 AUG 2019. See the end of the full text for details.

Increased Fall Precipitation in the Southeastern United States Driven by Higher-Intensity, Frontal Precipitation

Daniel A. Bishop^{1,2} , A. Park Williams¹ , and Richard Seager¹ 

¹Lamont-Doherty Earth Observatory, Columbia University, Palisades, NY, USA, ²Department of Earth and Environmental Sciences, Columbia University, New York, NY, USA

Abstract During 1895–2018, fall precipitation increased by nearly 40% in the southeastern United States north of the Gulf of Mexico due to increased circulation around the western North Atlantic Subtropical High, which enhanced moisture transports into the region. We find here that these increases in southeastern U.S. fall precipitation manifested almost entirely as increases in precipitation intensity, not frequency. Further, the enhanced moisture transports increased precipitation totals far more on the highest-intensity precipitation days than on the lower-intensity days, leading to nearly all of the increase to be delivered on extreme (top-5% intensity) precipitation days. Eighty-seven percent of the fall precipitation increase was driven by non-tropical storms (mostly frontal), not tropical cyclones, though the proportion of precipitation falling as either storm type did not change. Further research is needed to evaluate whether these observed precipitation increases are likely to continue, stabilize, or reverse.

Plain Language Summary Fall precipitation increased over the twentieth century in the southeastern United States due to increased wind-driven moisture transport from the Gulf of Mexico. Although fall is tropical cyclone (hurricane) season, it was non-tropical storms (mostly frontal) that dominated the precipitation increase. Further, the fall precipitation increase manifested as an increase in storm intensity, not frequency. The most intense 5% of non-tropical storms accounted for nearly three quarters of the increase in fall precipitation in the southeastern United States during 1895–2018. Climate models project that warming-induced humidity increases will also intensify storms, which would add to the wind-driven intensification detected thus far. If the observed wind-driven increase in intense precipitation continues and is added to by the effects of rising humidity, severe flooding from extreme frontal storms could become more common and severe in this region.

1. Introduction

The intensity and frequency of precipitation events increased across much of the contiguous United States during the 20th century, and these increases are projected to continue throughout the 21st century (Carter et al., 2018; DeGaetano, 2009; Easterling et al., 2017; Kunkel, 2003; Kunkel et al., 2003; Kunkel, Karl, et al., 2012; Singh et al., 2013; Villarini et al., 2012). Increases in precipitation intensity (Carter et al., 2018), precipitation frequency (Bishop & Pederson, 2015), streamflow (Allen & Ingram, 2002; Hayhoe et al., 2007), and flood occurrence (Mallakpour & Villarini, 2015) have also been observed across much of the contiguous United States. Future changes in precipitation intensity and frequency have important implications for flood risk (Milly et al., 2002), human health (Greenough et al., 2001), water resources (Alcamo et al., 2007), ecosystems (Reichstein et al., 2013), and agriculture (Rosenzweig et al., 2002).

Across much of the eastern United States, total annual precipitation increased during the 20th century (Hartmann et al., 2013; Pederson et al., 2013; Seager et al., 2012), largely driven by increases during the fall season (September–November; Easterling et al., 2017; Wang et al., 2009). In the southeastern United States, fall precipitation increased by nearly 40% during the 20th century and altered the region's annual cycle (Bishop et al., 2019; Williams et al., 2017). This increase in fall southeastern U.S. precipitation was driven by enhanced wind circulation around the western ridge of the North Atlantic Subtropical High, but the ultimate cause of this circulation change remains undiagnosed (Bishop et al., 2019). The means by which the fall precipitation increases in the southeastern United States manifested have also not been evaluated and key questions remain. For example, is increased fall precipitation in the southeastern United States related to tropical cyclones or extratropical storms? Are the increases a result of greater

storm frequency or increased precipitation intensity? Assessing the mechanisms of moisture delivery from transient (daily)-timescale weather systems could yield additional insight into the large-scale processes driving long-term fall wetting in the southeastern United States.

Fall-season extreme precipitation in the tropical and subtropical Atlantic basin is commonly associated with tropical cyclones given that the climatological peak of the Atlantic hurricane season occurs during August–October (Landsea, 1993; Moore et al., 2015). This tropical influence is strong along the Atlantic coast of the United States and in the southeastern United States north of the Gulf of Mexico where the frequency of U.S.-landfalling tropical cyclones is at its maximum (Khouakhi et al., 2017; Kunkel, Easterling, et al., 2012). The influence of tropical cyclones on extreme precipitation in the southeastern U.S. increased in the late 20th century, particularly along the Atlantic coast (Knight & Davis, 2009; Kunkel et al., 2010). Therefore, it is pertinent to investigate the influences of tropical cyclones versus non-tropical storm types (e.g., frontal) on southeastern U.S. fall precipitation. Storm-type classification has been broadly applied in synoptic meteorology and climatology research (e.g., Kunkel, Easterling, et al., 2012; Maxwell et al., 2017; Sheridan, 2002). Evaluating the historical contributions of storm types of varying intensities would provide valuable detail to our understanding of the large increases in fall precipitation that occurred in the southeastern United States over the past century.

Here, we investigate the influences of daily precipitation intensity, frequency, and storm type on the observed increases in fall precipitation in the southeastern United States during 1895–2018. Our analysis seeks to answer the following questions:

1. How did extreme precipitation affect the observed fall precipitation trend in the southeastern United States?
2. Did the observed fall precipitation trend in the southeastern United States align with a specific storm type such as tropical cyclones?

By addressing these questions, we gain a better understanding of how the observed increases in southeastern U.S. fall precipitation have been generated, which is critical to determine the ultimate causes and possible future trajectory of these trends.

2. Data and Methods

2.1. Study Region and Data

We define our study region as the southeast United States-Gulf of Mexico (SE-Gulf), a geographic box immediately north of the Gulf of Mexico (29 to 37°N, 98 to 84°W; see Figure 1a) that bounds the area with largest fall wetting trend in the contiguous United States (Bishop et al., 2019). Daily precipitation totals for 1895–2018 were derived from the U.S. subset of the daily Global Historical Climatology Network version 3.26 (GHCN; Menne et al., 2012). To ensure the stations represented a continuous record, weather stations were only included if, for at least 75% of 1895–2018 years, all three fall months (September–November) had valid observations of precipitation total on at least 95% of days. Ninety-nine stations met these criteria in the SE-Gulf region. To avoid biasing the regional mean toward areas with high station density, records were gridded by averaging across all station records within $2^\circ \times 2^\circ$ geographic boxes. A SE-Gulf regional mean record of daily precipitation total was then calculated using a land-area weighting among grid boxes. We also evaluated fall precipitation records using the monthly $1/24^\circ$ -gridded National Oceanic and Atmospheric Administration (NOAA) Climgrid dataset (Vose et al., 2014) to assure that the trends and interannual variability were consistent across data sets. Linear least squares trends in fall precipitation were calculated across the contiguous United States for Climgrid and across the southeastern U.S. study region for both GHCN and Climgrid.

To evaluate atmospheric circulation and precipitation efficiency (precipitation divided by precipitable water) for 1948–2018, we use daily gridded climate data from the National Center for Environmental Prediction and National Center for Atmospheric Research Reanalysis (NCEP-NCAR; Kalnay et al., 1996).

2.2. Influence of Storm Intensity

To address how the mean intensity and frequency of daily precipitation impacted fall precipitation trends during 1895–2018, we used the SE-Gulf regionally-averaged GHCN fall daily precipitation record to

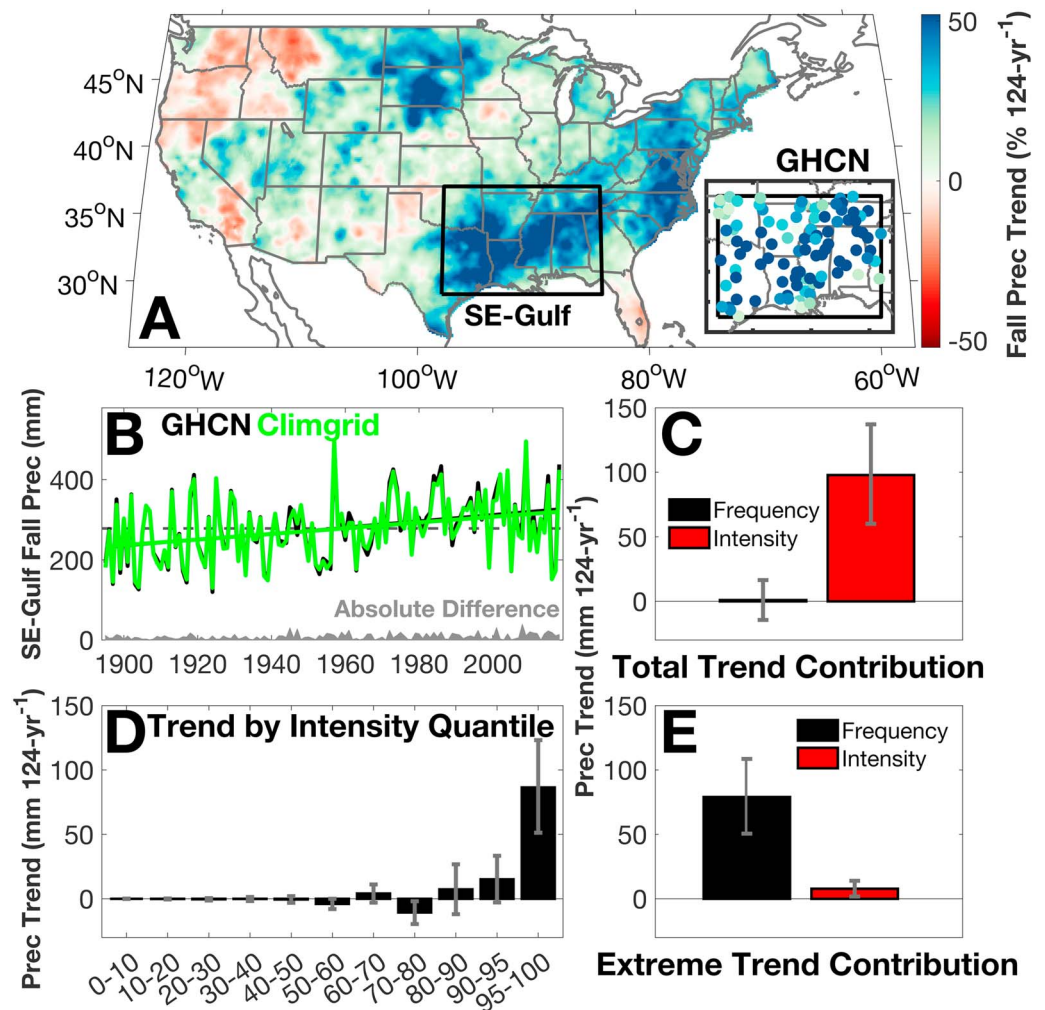


Figure 1. (a) 1895-2018 National Oceanic and Atmospheric Administration (NOAA) Climgrid fall precipitation trends (colors) with individual Global Historical Climatology Network (GHCN) trends (inset scatterplot). (b) Time series of fall SE-Gulf precipitation for Climgrid and GHCN, and the absolute difference between the two time series. (c) The contributions of the frequency (black) versus intensity (red) of daily precipitation to the 1895-2018 fall SE-Gulf precipitation trend. (d) Contributions from quantiles of daily precipitation totals to the trend. (e) Frequency (black) versus intensity (red) contributions of the most intense 5% of daily precipitation totals to the trend. Brackets bound 95% confidence intervals (c-e).

calculate fall frequency and intensity of daily measurable precipitation totals (>1 mm/day). For each individual fall season during 1895-2018, *frequency* is defined as the number of days with measurable precipitation and *mean intensity* is defined as the mean daily precipitation (intensity) on fall days with measurable precipitation. We then disaggregated fall precipitation totals into components driven by frequency or intensity, calculated annually as

$$P_{\text{int}} = \bar{f} * \text{int} \tag{1a}$$

$$P_{\text{f}} = \bar{f} * \overline{\text{int}}, \tag{1b}$$

where P_{int} is precipitation driven by intensity, P_{f} is precipitation driven by frequency, f is frequency of days with precipitation each fall, int is the mean daily precipitation total on days with precipitation each fall, and overbars indicate the 1895-2018 climatological fall mean. Linear trends for each component were calculated to evaluate how each component contributed to the long-term fall precipitation increase in the SE-Gulf. Trend significance was assessed using both the Mann-Kendall tau test and F statistic.

To investigate the contributions of changes in precipitation within different daily intensity classes, we separated days into nonoverlapping intensity deciles (0-10%, 10-20%, 20-30%, etc.) with the last decile further separated into 90-95% and 95-100%, where 95-100% represents the top-5% intensity for days with measurable precipitation (hereafter referred to as “extreme precipitation”). Total fall precipitation from each quantile was then summed for each year:

$$P_{yr,x-y\%} = \sum_{n=1}^{91} (P_{n,yr} | P_{x\%} < P_{n,yr} \leq P_{y\%}) \quad (2)$$

where $P_{yr,x-y\%}$ is total fall precipitation in quantile “x-y%” for year “yr” (e.g., $P_{1895,95-100\%}$ is total fall precipitation in quantile 95-100% for 1895), n is the sequential day during the fall season (e.g., $n=1$ is September 1 and $n=91$ is November 31), $P_{n,yr}$ is the precipitation total on day “n” in year “yr”, and $P_{x\%}$ and $P_{y\%}$ are daily precipitation quantile threshold values calculated from all daily precipitation totals during the fall season between 1895 and 2018. This calculation creates a time series during 1895-2018 of total fall precipitation resulting from daily precipitation for each intensity quantile. Linear trends were calculated to quantify the contribution of precipitation within each quantile to the total fall precipitation trend.

2.3. Influence of Storm Types

As tropical cyclones are common during the fall season in the southeastern United States (Kunkel, Easterling, et al., 2012), we disaggregated the fall precipitation record into contributions from tropical cyclones and non-tropical storms. Daily precipitation from tropical cyclones for 1895-2018 was defined using the revised Atlantic Hurricane Database (HURDAT2; Landsea et al., 2015). We defined tropical cyclones as tropical depressions, storms, and hurricanes, excluding other HURDAT2 classifications that included extratropical and subtropical cyclones and tropical waves. Following a modified approach from Kunkel, Easterling, et al. (2012), tropical cyclone days were categorized when a tropical cyclone’s minimum central pressure was within 5° in both latitude and longitude from the SE-Gulf bounding box. The remaining days with measurable precipitation were classified as non-tropical precipitation, which includes frontal, extratropical, and subtropical cyclones, and other classifications. To evaluate circulation anomalies associated with each storm type, daily NCEP-NCAR sea level pressure (SLP) and vertically-integrated surface-700 hPa moisture flux anomalies were averaged across tropical and non-tropical cyclone days (all and extreme precipitation days) during 1948-2018.

Although fall is the peak season for tropical cyclones, non-tropical frontal storm types have been shown to dominate fall precipitation in the southeastern United States (Kunkel, Easterling, et al., 2012; Maxwell et al., 2017). We classified frontal storm types following the methods in Text S1 in the supporting information. Daily NCEP-NCAR SLP and moisture flux anomalies were averaged across frontal days for comparison with anomalies on non-tropical precipitation days.

To evaluate the effects of each storm type on the fall precipitation trend, we calculated fall daily precipitation total, mean intensity, and frequency for each year from each storm type following the methods from section 2.2. Linear trends were then calculated for each subset to evaluate total contribution to the long-term (1895-2018) SE-Gulf fall precipitation increase.

3. Results and Discussion

3.1. Fall Precipitation and Influence of Storm Intensity

SE-Gulf fall precipitation computed from NOAA Climgrid increased by 37% (86 mm) and GHCN increased by 42% (97 mm) during 1895-2018 (Figures 1a and 1b). The fall precipitation trends were positive for all 99 GHCN stations, ranging from 2 to 131% (Figure S1 in the supporting information), indicating a coherent increase among the SE-Gulf stations with the longest and most complete precipitation records. The records of SE-Gulf regional fall precipitation total calculated from GHCN and Climgrid correlated strongly ($r = 0.99$). The GHCN record is used for the remainder of the analyses because they require daily precipitation totals.

After disaggregating the fall precipitation record into mean intensity and frequency contributions, mean intensity was the dominant driver (101%; 98 mm) of the linear increase during 1895-2018, with negligible contributions from frequency (1%; 1 mm) and interaction of intensity and frequency (-2%; -2 mm;

Figure 1c). The vast majority of these intensity-driven increases in SE-Gulf fall precipitation were driven by increases in the highest daily precipitation totals. This is consistent with the findings of Michaels et al. (2004), who evaluated relationships between precipitation intensity and trends in annual (not fall) precipitation totals. When partitioning SE-Gulf GHCN daily precipitation into intensity quantiles, the precipitation total on days with extreme precipitation (top-5%) had the strongest positive linear trend (86 mm), accounting for 89% of the total SE-Gulf fall precipitation trend. The remaining intensity quantiles had trends ranging from -11 mm (-11%; 70th-80th intensity percentiles) to 15 mm (16%; 90th-95th intensity percentiles; Figure 1d). Among extreme precipitation days (top-5%), an increase in extreme frequency was the primary driver of increased precipitation in this quantile (91%; 79 mm), while mean intensity contributed to 9% (8 mm) of the increase (Figure 1e). These results indicate an increase in the number of precipitation days surpassing the top-5% intensity threshold.

While the number of extreme (top-5%) precipitation days in each fall season in the SE-Gulf increased from 1.7 to 5.7 days, a ~238% increase ($p < 0.05$), the total number of fall days with measurable precipitation did not change significantly ($p > 0.05$). The increase in precipitation did not occur as a consistent increase across all intensity classes, which would have manifested in Figure 1c as a decrease in the lowest intensity classes to account for the increase in the higher intensity classes. Instead, the increases in precipitation intensity predominantly occurred among the highest-intensity days (Figure S2), indicating that the increase in SE-Gulf fall precipitation occurred due to an intensification of the strongest storms.

Bishop et al. (2019) demonstrated that the increase in SE-Gulf fall precipitation was due to a mean-state increase in low-level southerly moisture transport due to enhanced southerly wind from the Gulf of Mexico. Given our results here, it becomes essential to address why a mean-state increase in moisture transport would increase precipitation for the most intense storms. To investigate, we calculated regionally-averaged daily 1948-2018 NCEP-NCAR vertically-integrated meridional moisture flux over the Gulf of Mexico (29 to 21°N, 98 to 84°W; see Bishop et al., 2019, for methods) and separated into moisture flux quantiles (most southerly: 90-100%, most northerly: 0-10%). We then calculated the median and interquartile range of precipitation totals, column-total precipitable water, and precipitation efficiency for days within each moisture flux quantile. The same calculation was made for precipitation efficiency estimates partitioned by precipitable water quantiles.

As southerly moisture flux from the Gulf of Mexico increases, SE-Gulf fall daily precipitation intensity responds exponentially, while the amount of SE-Gulf precipitable water increases logarithmically (Figures 2a and 2b). This suggests that as moisture flux into the SE-Gulf increases and relative humidity rises, so does the proportion of water vapor that is converted to precipitation. Confirming this relationship, precipitation efficiency in the SE-Gulf increases linearly in response to southerly moisture flux and precipitable water (Figures 2c and 2d), indicating that increased moisture flux into the SE-Gulf leads to both increased precipitable water *and* precipitation efficiency, which act together to amplify precipitation intensity.

3.2. Influence of Storm Types

We next investigated the impact of tropical cyclones and non-tropical storms on fall precipitation. Both storm types are associated with low-level moisture transport to the SE-Gulf region from the Gulf of Mexico. Composites of SLP on days when tropical cyclones caused SE-Gulf precipitation indicated cyclonic circulation around a low-pressure minimum in the northern Gulf of Mexico (Figure 3a). The horizontal SLP gradient and cyclonic circulation around the low-pressure minimum were strengthened during extreme tropical cyclone precipitation days (Figure 3b).

When tropical cyclones were not impacting the region, SE-Gulf precipitation was associated with a Rossby wave pattern across North America with low SLP anomalies across the eastern and midwestern United States, and high SLP anomalies in Nova Scotia and, to a lesser extent, the northwestern United States. This ridge-trough pattern drives southerly moisture flux anomalies from the Gulf of Mexico and moisture convergence in the SE-Gulf region (Figure 3c). This pattern was amplified during extreme precipitation days (Figure 3d). These non-tropical SLP composites feature strong horizontal gradients in SLP and surface temperature along warm or cold frontal boundaries. The majority of non-tropical total precipitation (67%) and days with precipitation (61%) were classified as frontal. Surface circulation composites of these frontal days

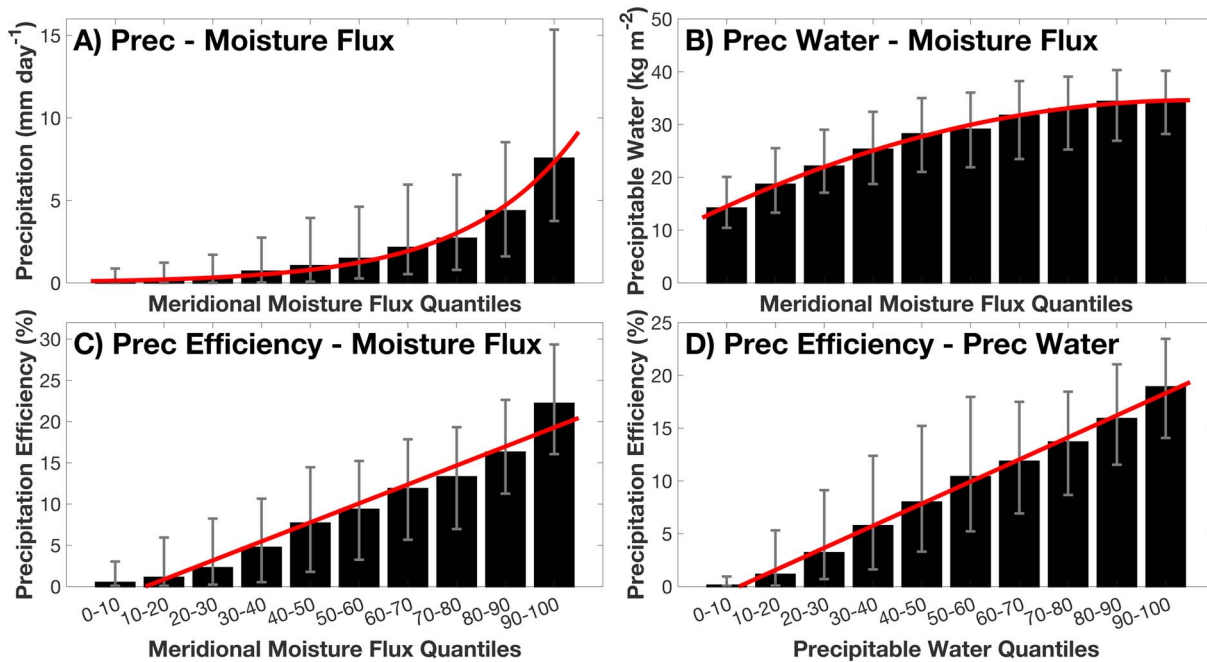


Figure 2. 1948-2018 SE-Gulf (a) Global Historical Climatology Network (GHCN) daily fall precipitation totals partitioned by quantiles of Gulf of Mexico daily vertically-integrated (surface-700 hPa) meridional moisture flux. (b) Column-total precipitable water partitioned by meridional moisture flux quantiles. (c and d) Precipitation efficiency partitioned by quantiles (x axis) of meridional moisture flux and precipitable water, respectively. Bars represent median daily precipitation for each quantile, brackets represent interquartile range, and red lines represent exponential (a), logarithmic (b), and linear (c and d) fits to medians. For meridional moisture flux, the largest quantiles represent the most positive southerly moisture flux values.

were nearly identical to those of non-tropical precipitation days (Figures S3 and 3c and 3d). This is consistent with the dominance of frontal storm types in the fall precipitation climatology (Kunkel, Easterling, et al., 2012) and rapid drought cessation from high-intensity precipitation events (Maxwell et al., 2017) in the southeastern United States.

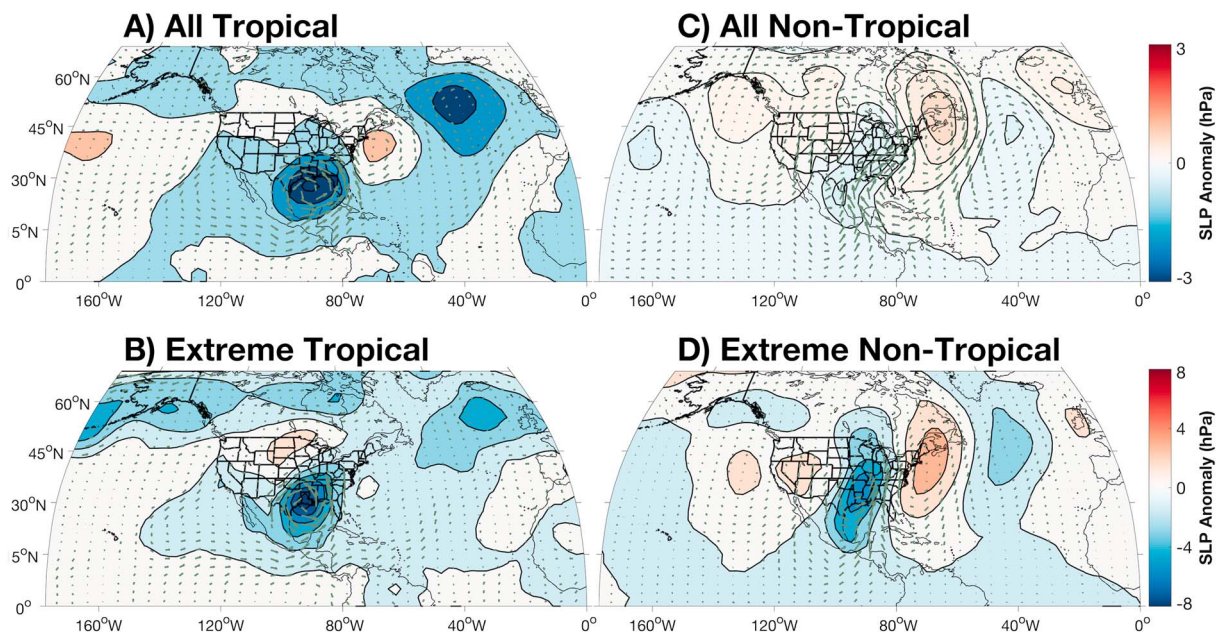


Figure 3. Composite maps of 1948-2018 National Center for Environmental Prediction-National Center for Atmospheric Research (NCEP-NCAR) sea-level pressure (colors) and surface-700 hPa vertically-integrated moisture flux (vectors) anomalies for days with measurable precipitation from (a and b) tropical cyclones or (c and d) non-tropical events during all days (a and c) and top-5% intensity days (b and d).

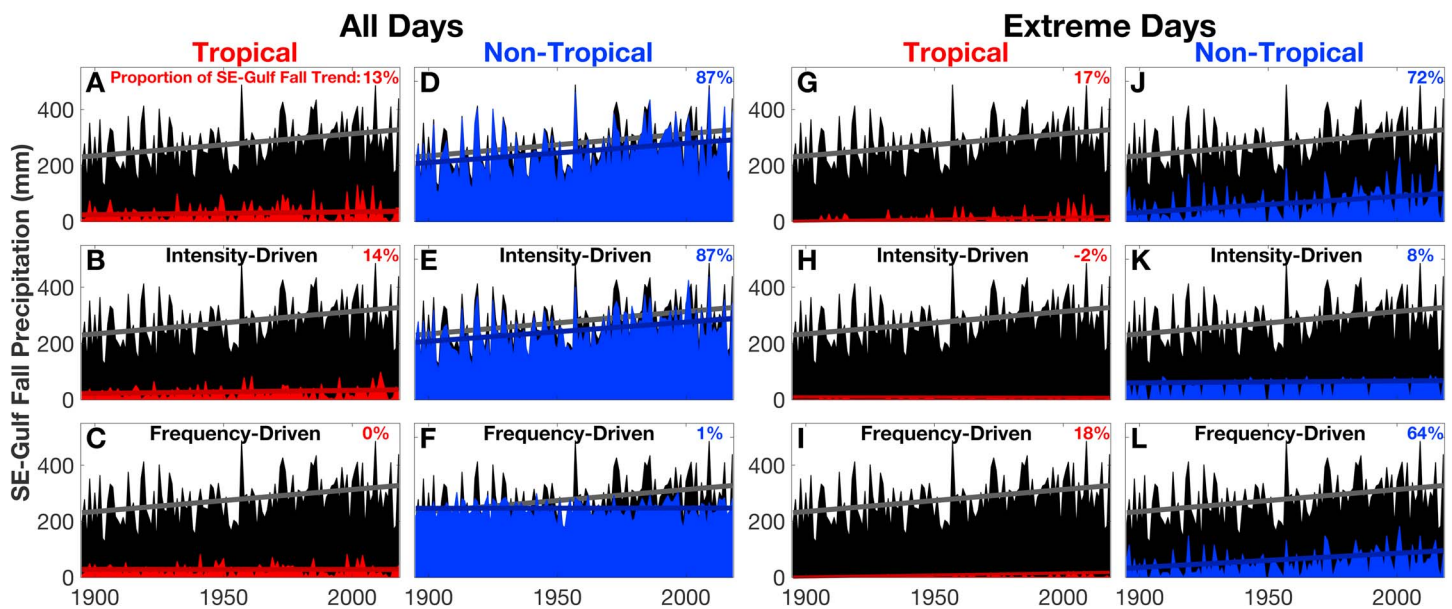


Figure 4. 1895-2018 SE-Gulf fall precipitation contributions from (a-f) all and (g-l) extreme tropical cyclone (first and third columns) and nontropical (second and fourth columns) days for total (top row), mean intensity-driven (middle row), and frequency-driven (bottom row) precipitation. Fall precipitation from tropical cyclones and non-tropical storms are shown in red and blue, respectively. Total fall precipitation from *all storm types* is shown in black and is common to all panels. Linear regressions are thick lines.

Despite the fact that fall is the peak tropical cyclone season in the SE-Gulf, tropical cyclones did not dominate the fall precipitation record. Non-tropical precipitation constituted the vast majority of the *total* SE-Gulf fall precipitation during 1895-2018, accounting for 89% of the total fall precipitation and 91% of the frequency of precipitation days during 1895-2018. During 1948-2018, 60% (56%) of total fall precipitation (frequency) was frontal, 11% (9%) was tropical, and 29% (35%) was not classified as either tropical or frontal. In terms of linear trend contribution, tropical cyclone precipitation only accounted for 13% of the total SE-Gulf fall precipitation increase (Figure 4a), which was primarily driven by mean intensity (14% of fall precipitation trend) rather than frequency (<1%; -1% from interaction; Figures 4b and 4c and S4). Non-tropical precipitation accounted for the other 87% of the fall precipitation trend (Figure 4d). This increase in non-tropical precipitation was also primarily driven by mean intensity (87%) rather than frequency (<1%; Figures 4e and 4f and S4). These results indicate that the increase in SE-Gulf fall precipitation has come about largely as an increase in the intensity of non-tropical (mostly frontal) precipitation events. Importantly, the proportion of precipitation occurring in non-tropical versus tropical storms had no trend during 1895-2018. This suggests that the larger increase in non-tropical precipitation arose simply because non-tropical precipitation totals are climatologically much higher than tropical precipitation totals in fall.

Next, given the increase in fall extreme precipitation, we evaluated the role of the *most extreme* storm types in driving the SE-Gulf fall precipitation trend. Extreme tropical cyclone precipitation accounted for 17% of the total fall precipitation trend (Figure 4g) and accounted for all of the increased precipitation caused by tropical cyclones (Figure 4a). This increase in extreme tropical cyclone precipitation was primarily driven by an increase in the frequency of the most intense tropical cyclones (18% of fall precipitation trend) rather than an increase in the intensity of these storms (-2%; 1% from interaction; Figures 4h and 4i and S4). Extreme non-tropical precipitation accounted for nearly three quarters of the fall precipitation trend (72%; Figure 4j), also primarily driven by increased frequency of intense non-tropical events (64%) rather than an increase in the intensity of these events (8%; Figures 4k and 4l). These results indicate that the SE-Gulf fall precipitation increase has been predominantly driven by increases in extreme non-tropical (mostly frontal) precipitation events. This is consistent with the climatologically high proportion of frontal storm types among extreme precipitation events in midlatitude regions (Catto & Pfahl, 2013).

4. Conclusions

Substantial increases in southeastern U.S. fall precipitation during 1895–2018 were driven mostly by increased precipitation intensity, with little change in the number of precipitating days. The increase in precipitation intensity occurred as an intensification of the strongest storms leading to more precipitation events exceeding the extreme (top 5%) threshold. Despite fall being tropical cyclone season, the intensified precipitation events that led to the increase in fall precipitation total were mostly frontal storms. Tropical cyclone intensity also increased slightly, however. Our previous research indicates that the observed increases in non-tropical precipitation intensity that we report here have been driven mainly by enhanced mean atmospheric circulation around the western ridge of the North Atlantic Subtropical High, which led to increased moisture transports into the southeastern United States from the Gulf of Mexico (Bishop et al., 2019). Our findings here provide further insight into how increased southerly moisture transports from the Gulf of Mexico have manifested as increases in southeastern U.S. fall precipitation.

It remains to be seen whether the observed increases in extreme southeastern U.S. fall precipitation will continue, level off, or reverse direction in the coming years. Model projections suggest that anthropogenic climate change should enhance southeastern U.S. fall extreme precipitation over the next century, but with relatively little change in total fall precipitation (Singh et al., 2013). Continued increases in frequency and intensity of extreme precipitation combined with projected increases in daily dry extremes (Singh et al., 2013) could lead to an increased potential for costly and life-threatening floods in the southeastern United States (Trenberth et al., 2003). The effects of extreme precipitation on flood risk are highly complex and may be most potent in small-to-medium sized runoff basins that can be highly affected by single events (Kunkel et al., 1999). The most severe flood events in the southeastern United States are often associated with tropical cyclones, such as Hurricane Harvey in 2017 (Emanuel, 2017; van Oldenborgh et al., 2017). However, non-tropical (mostly frontal) systems compose the vast majority of the southeastern U.S. fall precipitation in terms of both total precipitation and number of storms. It is therefore reasonable to suspect that continued intensification of non-tropical storms would enhance the risk of severe flooding as extreme precipitation totals become more commonplace among already frequently observed frontal storm types. While the thermodynamic (humidity-driven) contribution to the southeastern U.S. fall precipitation trend has been small relative to the dynamic (wind-driven) contribution (Bishop et al., 2019), the projected warming-induced increase in atmospheric moisture content is expected to amplify extreme precipitation increases globally (Allan & Soden, 2008). In the southeastern United States, models do project daily precipitation extremes to intensify due to anthropogenic warming (Pendergrass et al., 2017), but the observed, circulation-driven increases in fall precipitation in this region far exceed simulated trends (Bishop et al., 2019). Should the as-yet undiagnosed circulation-driven increases in extreme precipitation continue, and if these co-occur with model-projected increases in extreme precipitation that is driven by increases in humidity, it follows that the resultant increases in storm intensity could increase flood risk beyond that which may be inferred from current climate-model projections of precipitation. Further research is needed to understand the drivers of the observed enhancement in large-scale circulation around the western ridge of the North Atlantic Subtropical High. Such an understanding is critical to accurately characterize the roles of natural versus anthropogenic climate variability in southeastern U.S. hydroclimate and anticipate the full range of variability of hydrological extremes in this flood-prone region.

Acknowledgments

This research was supported by the NASA Earth and Space Science Graduate Student Fellowship (80NSSC17K0402), the National Science Foundation (AGS-1703029 and AGS-1401400), and NOAA award NA17OAR4310126. We thank Arlene Fiore, Edward Cook, and two reviewers for feedback that improved the manuscript. Climate data from this study are publicly available in their existing repositories for NOAA Climgrid (<ftp://ftp.ncdc.noaa.gov/pub/data/climgrid/>), GHCN (<https://www.ncdc.noaa.gov/ghcn-daily-description>), HURDAT2 (http://www.aoml.noaa.gov/hrd/hurdat/Data_Storm.html), and NCEP-NCAR (<https://www.esrl.noaa.gov/psd/data/gridded/data.ncep.reanalysis.html>). Lamont contribution 8834.

References

- Alcamo, J., Flörke, M., & Märker, M. (2007). Future long-term changes in global water resources driven by socio-economic and climatic changes. *Hydrological Sciences Journal*, 52(2), 247–275. <https://doi.org/10.1623/hysj.52.2.247>
- Allan, R. P., & Soden, B. J. (2008). Atmospheric warming and the amplification of precipitation extremes. *Science*, 321(5895), 1481–1484. <https://doi.org/10.1126/science.1160787>
- Allen, M. R., & Ingram, W. J. (2002). Constraints on future changes in climate and the hydrologic cycle. *Nature*, 419(6903), 228–232. <https://doi.org/10.1038/nature01092>
- Bishop, D. A., & Pederson, N. (2015). Regional variation of transient precipitation and rainless-day frequency across a subcontinental hydroclimate gradient. *Journal of Extreme Events*, 02(02), 1550007. <https://doi.org/10.1142/S2345737615500074>
- Bishop, D. A., Williams, A. P., Seager, R., Fiore, A. M., Cook, B. I., Mankin, J. S., et al. (2019). Investigating the causes of increased twentieth-century fall precipitation over the southeastern United States. *Journal of Climate*, 32(2), 575–590. <https://doi.org/10.1175/JCLI-D-18-0244.1>
- Carter, L., Terando, A., Dow, K., Hiers, K., Kunkel, K. E., Lascrain, A., et al. (2018). In D. R. Reidmiller, et al. (Eds.), *Southeast. In Impacts, Risks, and Adaptation in the United States: Fourth National Climate Assessment* (Vol. II, pp. 743–808). Washington, DC, USA: U.S. Global Change Research Program. <https://doi.org/10.7930/NCA4.2018.CH19>

- Catto, J. L., & Pfahl, S. (2013). The importance of fronts for extreme precipitation. *Journal of Geophysical Research: Atmospheres*, *118*, 10,791–10,801. <https://doi.org/10.1002/jgrd.50852>
- DeGaetano, A. T. (2009). Time-dependent changes in extreme-precipitation return-period amounts in the continental United States. *Journal of Applied Meteorology and Climatology*, *48*(10), 2086–2099. <https://doi.org/10.1175/2009JAMC2179.1>
- Easterling, D. R., Kunkel, K. E., Arnold, J. R., Knutson, T., LeGrande, A. N., Leung, L. R., et al. (2017). In D. J. Wuebbles, et al. (Eds.), *Precipitation change in the United States. Climate Science Special Report: Fourth National Climate Assessment* (Vol. I, pp. 207–230). Washington, DC, USA: U.S. Global Change Research Program. <https://doi.org/10.7930/J0H993CC>
- Emanuel, K. (2017). Assessing the present and future probability of Hurricane Harvey's rainfall. *Proceedings of the National Academy of Sciences*, *114*(48), 12,681–12,684. <https://doi.org/10.1073/pnas.1716222114>
- Greenough, G., McGeehin, M., Bernard, S. M., Tritanji, J., Riad, J., & Engelberg, D. (2001). The potential impacts of climate variability and change on health impacts of extreme weather events in the United States. *Environmental Health Perspectives*, *109*(suppl 2), 191–198. <https://doi.org/10.1289/ehp.109-1240666>
- Hartmann, D. L., Tank, A. M. G. K., Rusticucci, M., Alexander, L. V., Brönnimann, S., Charabi, Y. A. R., et al. (2013). Observations: Atmosphere and surface. In *Climate Change 2013 the Physical Science Basis: Working Group I Contribution to the Fifth Assessment Report of the Intergovernmental Panel on Climate Change* (pp. 159–254). Cambridge: Cambridge University Press. <https://doi.org/10.1017/CBO9781107415324.008>
- Hayhoe, K., Wake, C. P., Huntington, T. G., Luo, L., Schwartz, M. D., Sheffield, J., et al. (2007). Past and future changes in climate and hydrological indicators in the US Northeast. *Climate Dynamics*, *28*(4), 381–407. <https://doi.org/10.1007/s00382-006-0187-8>
- Kalnay, E., Kanamitsu, M., Kistler, R., Collins, W., Deaven, D., Gandin, L., et al. (1996). The NCEP/NCAR 40-year reanalysis project. *Bulletin of the American Meteorological Society*, *77*(3), 437–471. [https://doi.org/10.1175/1520-0477\(1996\)077<0437:TNYRP>2.0.CO;2](https://doi.org/10.1175/1520-0477(1996)077<0437:TNYRP>2.0.CO;2)
- Khoulakhi, A., Villarini, G., & Vecchi, G. A. (2017). Contribution of tropical cyclones to rainfall at the global scale. *Journal of Climate*, *30*(1), 359–372. <https://doi.org/10.1175/JCLI-D-16-0298.1>
- Knight, D. B., & Davis, R. E. (2009). Contribution of tropical cyclones to extreme rainfall events in the southeastern United States. *Journal of Geophysical Research*, *114*, D23102. <https://doi.org/10.1029/2009JD012511>
- Kunkel, K. E. (2003). North American trends in extreme precipitation. *Natural Hazards*, *29*(2), 291–305. <https://doi.org/10.1023/A:1023694115864>
- Kunkel, K. E., Andsager, K., & Easterling, D. R. (1999). Long-term trends in extreme precipitation events over the conterminous United States and Canada. *Journal of Climate*, *12*(8), 2515–2527. [https://doi.org/10.1175/1520-0442\(1999\)012<2515:LTTIEP>2.0.CO;2](https://doi.org/10.1175/1520-0442(1999)012<2515:LTTIEP>2.0.CO;2)
- Kunkel, K. E., Easterling, D. E., Kristovich, D. A. R., Gleason, B., Stoecker, L., & Smith, R. (2010). Recent increases in U.S. heavy precipitation associated with tropical cyclones. *Geophysical Research Letters*, *37*, L24706. <https://doi.org/10.1029/2010GL045164>
- Kunkel, K. E., Easterling, D. E., Kristovich, D. A. R., Gleason, B., Stoecker, L., & Smith, R. (2012). Meteorological causes of the secular variations in observed extreme precipitation events for the conterminous United States. *Journal of Hydrometeorology*, *13*(3), 1131–1141. <https://doi.org/10.1175/JHM-D-11-0108.1>
- Kunkel, K. E., Easterling, D. R., Redmond, K., & Hubbard, K. (2003). Temporal variations of extreme precipitation events in the United States: 1895–2000. *Geophysical Research Letters*, *30*(17), 1900. <https://doi.org/10.1029/2003GL018052>
- Kunkel, K. E., Karl, T. R., Brooks, H., Kossin, J., Lawrimore, J. H., Arndt, D., et al. (2012). Monitoring and understanding trends in extreme storms: State of knowledge. *Bulletin of the American Meteorological Society*, *94*(4), 499–514. <https://doi.org/10.1175/BAMS-D-11-00262.1>
- Landsea, C., Franklin, J., & Beven, J. (2015). The revised Atlantic Hurricane Database (HURDAT2). United States National Oceanic and Atmospheric Administration's National Weather Service, accessed 17 May 2019. [Available at http://www.aoml.noaa.gov/hrd/hurdat/Data_Storm.html]
- Landsea, C. W. (1993). A climatology of intense (or major) Atlantic hurricanes. *Monthly Weather Review*, *121*(6), 1703–1713. [https://doi.org/10.1175/1520-0493\(1993\)121<1703:ACOIMA>2.0.CO;2](https://doi.org/10.1175/1520-0493(1993)121<1703:ACOIMA>2.0.CO;2)
- Mallakpour, I., & Villarini, G. (2015). The changing nature of flooding across the central United States. *Nature Climate Change*, *5*(3), 250–254. <https://doi.org/10.1038/nclimate2516>
- Maxwell, J. T., Knapp, P. A., Ortegren, J. T., Ficklin, D. L., & Soulé, P. T. (2017). Changes in the mechanisms causing rapid drought cessation in the southeastern United States. *Geophysical Research Letters*, *44*, 12,476–12,483. <https://doi.org/10.1002/2017GL076261>
- Menne, M. J., Durre, I., Korzeniewski, B., McNeal, S., Thomas, K., Yin, X., et al. (2012). Global Historical Climatology Network-Daily (GHCN-Daily), Version 3.26. NOAA National Climatic Data Center, accessed 06 May 2019. <http://doi.org/10.7289/V5D21VHZ>
- Michaels, P. J., Knappenberger, P. C., Frauenfeld, O. W., & Davis, R. E. (2004). Trends in precipitation on the wettest days of the year across the contiguous USA. *International Journal of Climatology*, *24*(15), 1873–1882. <https://doi.org/10.1002/joc.1102>
- Milly, P. C. D., Wetherald, R. T., Dunne, K. A., & Delworth, T. L. (2002). Increasing risk of great floods in a changing climate. *Nature*, *415*(6871), 514–517. <https://doi.org/10.1038/415514a>
- Moore, B. J., Mahoney, K. M., Sukovich, E. M., Cifelli, R., & Hamill, T. M. (2015). Climatology and environmental characteristics of extreme precipitation events in the southeastern United States. *Monthly Weather Review*, *143*(3), 718–741. <https://doi.org/10.1175/MWR-D-14-00065.1>
- Pederson, N., Bell, A. R., Cook, E. R., Lall, U., Devineni, N., Seager, R., et al. (2013). Is an epic pluvial masking the water insecurity of the greater New York City region? *Journal of Climate*, *26*(4), 1339–1354. <https://doi.org/10.1175/JCLI-D-11-00723.1>
- Pendergrass, A. G., Knutti, R., Lehner, F., Deser, C., & Sanderson, B. M. (2017). Precipitation variability increases in a warmer climate. *Scientific Reports*, *7*(1), 17966. <https://doi.org/10.1038/s41598-017-17966-y>
- Reichstein, M., Bahn, M., Ciais, P., Frank, D., Mahecha, M. D., Seneviratne, S. I., et al. (2013). Climate extremes and the carbon cycle. *Nature*, *500*(7462), 287–295. <https://doi.org/10.1038/nature12350>
- Rosenzweig, C., Tubiello, F. N., Goldberg, R., Mills, E., & Bloomfield, J. (2002). Increased crop damage in the US from excess precipitation under climate change. *Global Environmental Change*, *12*(3), 197–202. [https://doi.org/10.1016/S0959-3780\(02\)00008-0](https://doi.org/10.1016/S0959-3780(02)00008-0)
- Seager, R., Pederson, N., Kushnir, Y., Nakamura, J., & Jurburg, S. (2012). The 1960s drought and the subsequent shift to a wetter climate in the Catskill Mountains region of the New York City watershed. *Journal of Climate*, *25*(19), 6721–6742. <https://doi.org/10.1175/JCLI-D-11-00518.1>
- Sheridan, S. C. (2002). The redevelopment of a weather-type classification scheme for North America. *International Journal of Climatology*, *22*(1), 51–68. <https://doi.org/10.1002/joc.709>
- Singh, D., Tsiang, M., Rajaratnam, B., & Diffenbaugh, N. S. (2013). Precipitation extremes over the continental United States in a transient, high-resolution, ensemble climate model experiment. *Journal of Geophysical Research: Atmospheres*, *118*, 7063–7086. <https://doi.org/10.1002/jgrd.50543>

- Trenberth, K. E., Dai, A., Rasmussen, R. M., & Parsons, D. B. (2003). The changing character of precipitation. *Bulletin of the American Meteorological Society*, *84*(9), 1205–1218. <https://doi.org/10.1175/BAMS-84-9-1205>
- van Oldenborgh, G. J., van der Wiel, K., Sebastian, A., Singh, R., Arrighi, J., Otto, F., et al. (2017). Attribution of extreme rainfall from Hurricane Harvey, August 2017. *Environmental Research Letters*, *12*(12), 124009. <https://doi.org/10.1088/1748-9326/aa9ef2>
- Villarini, G., Smith, J. A., & Vecchi, G. A. (2012). Changing frequency of heavy rainfall over the central United States. *Journal of Climate*, *26*(1), 351–357. <https://doi.org/10.1175/JCLI-D-12-00043.1>
- Vose, R. S., Applequist, S., Squires, M., Durre, I., Menne, M. J., Williams, C. N., et al. (2014). Improved historical temperature and precipitation time series for U.S. climate divisions. *Journal of Applied Meteorology and Climatology*, *53*(5), 1232–1251. <https://doi.org/10.1175/JAMC-D-13-0248.1>
- Wang, H., Schubert, S., Suarez, M., Chen, J., Hoerling, M., Kumar, A., & Pegion, P. (2009). Attribution of the seasonality and regionality in climate trends over the United States during 1950–2000. *Journal of Climate*, *22*(10), 2571–2590. <https://doi.org/10.1175/2008JCLI2359.1>
- Williams, A. P., Cook, B. I., Smerdon, J. E., Bishop, D. A., Seager, R., & Mankin, J. S. (2017). The 2016 southeastern U.S. drought: An extreme departure from centennial wetting and cooling. *Journal of Geophysical Research: Atmospheres*, *122*, 10,888–10,905. <https://doi.org/10.1002/2017JD027523>

Erratum

In the originally published version of this article, equation (1b) was incorrect. This error has since been corrected, and the present version may be considered the authoritative version of record.